View metadata, citation and similar papers at core.ac.uk
brought to you by CORE
provided by CiteSeerX

Magnetic susceptibility measurements at high pressure using designer diamond anvils

D. D. Jackson,[a] C. Aracne-Ruddle, V. Malba, and S. T. Weir
Lawrence Livermore National Laboratory, University of California, P.O. Box 808, Livermore, California 94550

S. A. Catledge and Y. K. Vohra
Department of Physics, University of Alabama at Birmingham, Birmingham, Alabama 35294-1170

(Received 29 July 2002; accepted 2 December 2002)

High pressure magnetic susceptibility experiments can yield valuable insights into the changes in magnetic behavior and electron correlation properties which can accompany extreme compressions of matter. However, magnetic susceptibility experiments with ultrahigh pressure diamond anvil cells are extremely challenging due to the very small size of the high-pressure sample (≈75 μm diameter) and the difficulty of obtaining good coupling between the sample and the sensing coil. As a result, measurement sensitivity and poor signal-to-background ratios tend to be serious concerns which limit the applicability of these experiments. We present here a new approach to high-pressure ac magnetic susceptibility experiments that involve specially fabricated diamond anvils with diamond encapsulated sensing microcoils which are located just 10–20 μm from the high-pressure sample. We also present some test results taken with a gadolinium sample in order to demonstrate the viability of this high-pressure ac susceptibility technique. © *2003 American Institute of Physics.* [DOI: 10.1063/1.1544084]

I. INTRODUCTION

The experimental investigation of the physical properties of matter under extreme pressures is currently a very active field of research. Using high-pressure diamond anvil cells (DACs)[1,2] experimenters are now able to routinely study materials under ultrahigh static pressures exceeding 100 GPa. These experiments are valuable for investigating a number of interesting high-pressure phenomena such as pressure-induced transformations of the crystalline structure, pressure-induced insulator-to-metal transitions, and pressure-induced superconductivity.

The high transparency of single crystal diamond anvils to optical and x-ray wavelengths has enabled the easy adaptation of diamond anvil cells to a wide variety of optical and x-ray diagnostic probes. However, other types of high-pressure experiments are much more problematic. Although ultrahigh pressure experiments have also been performed using electrical conductivity[3,4] and magnetic susceptibility[5–8] techniques to pressures above 100 GPa, these types of experiments suffer from difficulties related to the very small size of the sample (typical dimension ≈75 μm or less) and its relative inaccessibility while it is being pressurized in a diamond anvil cell.

We present a new technique for high-pressure ac magnetic susceptibility measurements which is based on a recently developed high-pressure technology that enables us to custom fabricate diamond anvils for various types of high-pressure experiments. These ''designer'' diamond anvils feature thin-film metal circuits encased within the diamond anvil itself.[9–11]

II. DESIGNER DIAMOND ANVILS

A simplified schematic diagram of a designer anvil as it would be used in a diamond anvil cell is shown in Fig. 1. The designer anvil consists of a standard 1/3 carat diamond with a tungsten thin-film probe patterned on its surface using three-dimensional (3D) laser pantography and two-dimensional (2D) projection lithography,[12,13] followed by high quality epitaxial diamond chemical vapor deposition (CVD).[9] The laser pantography system patterns an electrodeposited photoresist on the steep walls of the anvil by translating the anvil with precision computer-controlled stages (x, y, z, and θ) under a focused ion-argon laser beam. An acousto-optic modulator (AOM) is used to rapidly turn the beam on and off in conjunction with the stage movements. The electrodeposited resist provides a uniform photoactive layer of 6–20 μm on conductive substrates regardless of their shape. Typical probe linewidths are 10–30 μm and probe thicknesses range from 0.2 to 0.7 μm. These line patterns extend from the 300 μm diam culet of the anvil, where the high-pressure sample is located, then down the side of the anvil to 125 μm×250 μm pads, which serve as connection points for external instrumentation. Ordinary 2D projection lithography cannot be used for patterning the anvil walls because of the depth of field created by the angle of the diamond facets. Projection lithography can be used to pattern the intricate magnetic susceptibility coils on the 300 μm diam culet region because it is relatively flat. This combined use of both lithographic techniques has proven to be versatile approach to the problem of patterning nonflat surfaces.

[a]Electronic mail: djackson@mailaps.org

 © 2003 American Institute of Physics

Downloaded 04 Apr 2003 to 128.115.60.31. Redistribution subject to AIP license or copyright, see http://ojps.aip.org/rsio/rsicr.jsp

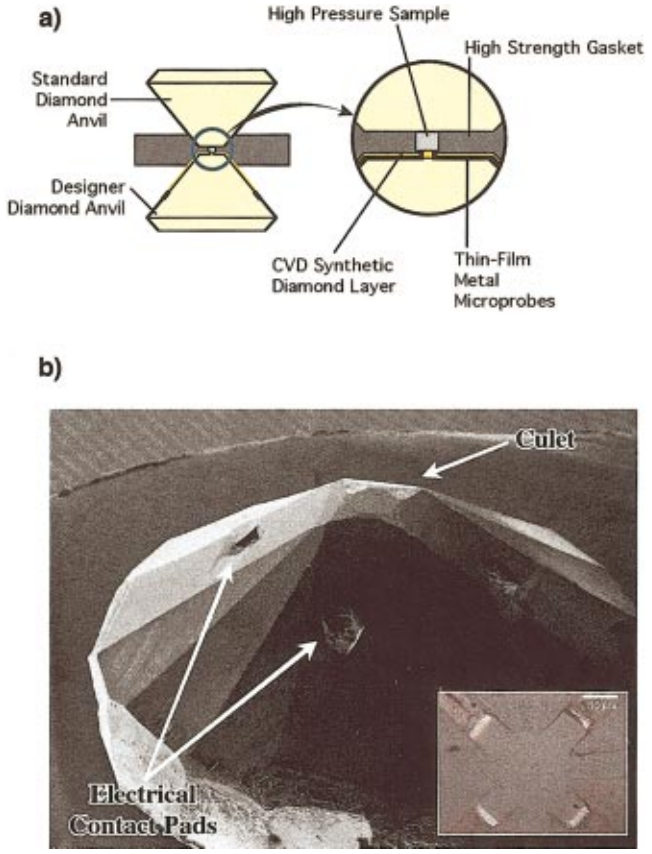

FIG. 1. (Color) (a) Simplified schematic diagram of a designer diamond anvil used for electrical resistivity measurements. Ultrahigh sample pressures are generated by forcing the two anvils together. The magnified view shows the high-pressure region between the two anvils. The designer anvil features a set of thin-film metal microprobes and a protective chemical vapor deposited diamond layer (shown in orange) encasing the microprobes. (b) Scanning electron micrograph (SEM) of a designer diamond anvil. Thin-film tungsten probes under the diamond surface extend from the electrical contact pads up to the culet where the high-pressure sample is located. The inset shows a magnified view of the probes emerging from the culet.

After fabrication of the tungsten microprobes, a single crystal layer of epitaxial diamond is deposited onto the anvil substrate by microwave plasma CVD using a 2% methane in hydrogen gas mixture. The typical as-grown diamond film thickness is about 20–50 μm. Finally, the rough as-grown diamond surface on the culet of the anvil is polished to a smooth finish to prepare for high-pressure experiments. Due to the homoepitaxial nature of the diamond film growth, the tungsten microprobes become fully integrated into the new single crystal designer diamond anvil, and are thus protected from damage due to shearing or abrasion in high-pressure experiments. These probes have been demonstrated to remain functional to 180 GPa.[9]

Taking advantage of the design flexibility afforded by the lithographic fabrication of the microprobe features, we report on a new class of designer anvils for high sensitivity ac magnetic susceptibility experiments which feature magnetic sensing coils embedded within the diamond. The culet of a designer diamond anvil used for ac susceptibility is shown in Fig. 2. The microcoil pattern on the culet consists of a five-turn coil with 5 μm linewidth, which can be seen after the lithography in Fig. 2(a). Figure 2(b) shows the culet

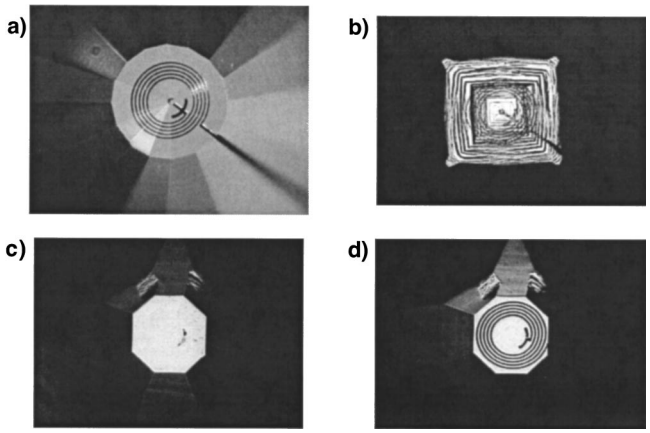

FIG. 2. Five-turn multiloop designer anvil (a) after lithographic fabrication of the microcoils, (b) immediately after CVD diamond encapsulation, and after an epitaxial CVD diamond layer has been deposited and polished, (c) viewed with reflected light and (d) transmitted light. The microcoil linewidth is 5 μm, and the coil pattern has outer and inner diameters of 210 and 120 μm, respectively. The diameter of the original diamond culet is 300 μm.

immediately after the CVD diamond encapsulation, which shows the rough growth steps which occur during the CVD process. The final step involves polishing the diamond down to micron tolerances in order to expose the arc at the inner microloop which can then make electrical contact with the metal gasket. Figure 2(c) shows the culet viewed with reflected light, in which only the exposed inner arc is observable, and Fig. 2(d) shows the same culet viewed with transmitted light in order to see the five-turn microcoil. Due to the close placement of this microcoil to the high-pressure sample, very high signal sensitivities and signal-to-background ratios are possible in high-pressure ac magnetic susceptibility experiments.

A. ac magnetic susceptibility with DACs

An ac magnetic susceptibility experiment is performed by creating a time varying magnetic field using an excitation coil and measuring the sample response by detecting the voltage induced in a sensing coil. The sensing coil is placed as close to the sample as possible in order to maximize the sensitivity. Any changes in the magnetic susceptibility of the sample alter the magnetic field lines and the amount of magnetic flux passing through the sensing coil, resulting in a change in the voltage induced.

A key concern in an ac magnetic susceptibility experiment is the degree of coupling between the sample and the sensing coil. Since the magnetic field from a magnetic dipole moment decreases as $1/r^3$, where r is the distance from the dipole, it is highly desirable to place the magnetic sensing coil as close as possible to the sample in order to achieve maximum possible sensitivity and signal-to-background ratio. Unfortunately, in a DAC experiment the sample is sandwiched between two diamond anvils, making it somewhat inaccessible. Therefore, high-pressure ac magnetic susceptibility experiments with DACs generally utilize sensing coils that are wrapped around the exteriors of the diamond anvils.[5,14,15] This approach, however, sacrifices a large amount of sensitivity since the filling factor of the sensing coil (i.e., the effective volume fraction of the coil filled by

Downloaded 04 Apr 2003 to 128.115.60.31. Redistribution subject to AIP license or copyright, see http://ojps.aip.org/rsio/rsicr.jsp

the sample), is very small. For example, a typical high-pressure sample may be only about 75 μm in diameter, while the external sensing coil may be 2–4 mm in diameter. The induced voltage generated by this sensing coil is predominantly due to the large, time-varying background magnetic flux from the excitation coil. The signal of interest, however, is the relatively small time-varying magnetic flux from the sample itself, which is superimposed onto the large excitation coil background. For example, the signal from a 100 μm diam superconducting sample may only be 100 nV and superimposed on a background signal of about 1 V for an uncompensated sensing coil,[5] a raw signal-to-background ratio of 10^{-7}. Thus, extreme care must be taken to cancel out the large background signal voltage with counterwound compensating coils and/or compensating circuits in order to recover signals from just the sample itself.

B. ac magnetic susceptibility with designer anvils

We now explore some of the performance and design issues associated with the microcoil designer anvil approach with the following calculations. For simplicity, we will assume a point magnetic dipole approximation for the induced ac magnetic moment of the sample. The magnetic field $\mathbf{B}_{\mathrm{dip}}$ due to the sample is then given by

$$\mathbf{B}_{\mathrm{dip}}=\frac{3\hat{r}_0(\hat{r}_0\cdot\mathbf{m})-\mathbf{m}}{r^3}, \tag{1}$$

where $\mathbf{m}$ is the magnetic dipole moment, r is the position where $\mathbf{B}_{\mathrm{dip}}$ is measured with respect to the sample, and $\hat{r}_0$ is the unit vector of r. This induced magnetic field from the sample is superimposed on the excitation field $\mathbf{B}_0=B_0\hat{z}$ so that the total magnetic flux captured by a coil of area A is then given by

$$\phi_{\mathrm{total}}=\int_A \mathbf{B}_{\mathrm{total}}\cdot\hat{n}ds=\int_A \mathbf{B}_0\cdot\hat{n}ds+\int_A \mathbf{B}_{\mathrm{dip}}\cdot\hat{n}ds. \tag{2}$$

We call the first term the background flux $\phi_B(=B_0A)$ and the second term the magnetic dipole flux ϕ_{dip}. If we assume that coil area A is normal to the $\mathbf{m}$ vector and located a distance d from point magnetic dipole, then ϕ_{dip}, given by the surface integral of $\mathbf{B}_{\mathrm{dip}}\cdot\hat{n}$ over coil area A, is

$$\phi_{\mathrm{dip}}=m\int_0^R \frac{2d^2-r^2}{(d^2+r^2)^{5/2}}dr=\frac{2\pi mR^2}{(d^2+R^2)^{3/2}}, \tag{3}$$

where R is the radius of the coil. For purposes of comparison, assume that we have a sensing coil external to the diamond anvils with $R=2$ mm that it is positioned at axial distance $d=0.5$ mm from the sample. Then, for a single-turn external coil, $\phi_{\mathrm{dip}}=2.87m\,(\mathrm{mm}^{-1})$, where m is the induced magnetic moment of the sample. On the other hand, for a diamond-encapsulated microcoil, the characteristic radius R is around 0.1 mm and the axial distance d may be about $\approx$0.02 mm. Thus, for a single-turn microcoil, $\phi_{\mathrm{dip}}=59.24m\,(\mathrm{mm}^{-1})$, and each turn captures about 20 times more flux than each turn of an external coil (Fig. 3).

A key concern is the magnitude of the background voltage, which is proportional to $\phi_B=B_0A$, in relation to the signal voltage. For a single-turn external coil with the dimensions already described, $\phi_B=4\pi B_0\,(\mathrm{mm}^2)$. For a single-turn microcoil ($R=0.1$ mm, $d=0.02$ mm), $\phi_B=0.01\pi B_0\,(\mathrm{mm}^2)$. Therefore, each turn of a microcoil captures only about 1/400 of the background flux of the external coil.

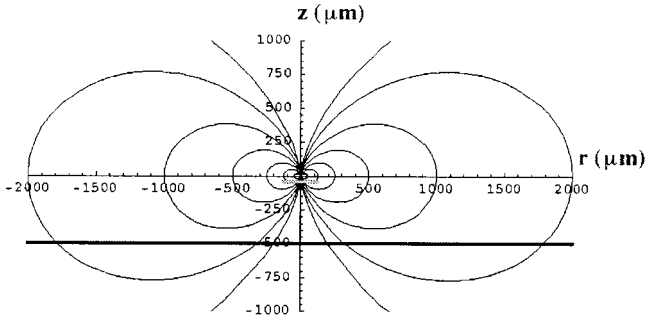

FIG. 3. Plot of the magnetic field lines from a point magnetic dipole. The axes are in μm. The magnetic dipole is located at the origin of the plot, and the dark solid lines at $y=-20$ and -500 μm represent a microcoil and the external coil described in the text, respectively. Due to its closeness to the sample, the microcoil captures approximately 20 times as much flux from the sample as the larger external coil while at the same time capturing only about 1/400 of the background flux from the excitation coil.

The signal voltage, proportional to ϕ_{dip}, is therefore about 20 times larger for a single-turn microcoil compared to a single-turn 2 mm external coil. Thus, our standard five-turn microcoil design captures approximately as much flux as a 100-turn external coil. Since hundreds of turns are often used for external sensing coils, the signal voltages from the microcoils can be expected to be comparable to, but somewhat smaller than, those of typical external sensing coils. However, the primary concern with high-pressure magnetic susceptibility experiments is generally not the magnitude of the signal voltage, but rather its level relative to the normally enormous background voltage, i.e., the signal-to-background ratio. We can estimate the relative intrinsic signal-to-background ratios by comparing the flux ratios $\phi_{\mathrm{dip}}/\phi_B$. For an external 2 mm coil, this ratio is $0.228(m/B_0)\,(\mathrm{mm}^{-3})$, but for a microcoil, the ratio is $1885.67(m/B_0)\,(\mathrm{mm}^{-3})$, an improvement of almost 10^4. Note that these flux ratios $\phi_{\mathrm{dip}}/\phi_B$ are independent of the number of turns in the coils, so increasing the number of turns does not increase the signal-to-background ratio.

III. EXPERIMENTAL DESCRIPTION

A. Circuit description

A schematic diagram of our diamond anvils and coil system is shown in Fig. 4. The excitation coil consists of approximately 55 turns of 32 AWG copper wire, and is wrapped around a standard diamond anvil. The sample, with typical starting dimensions of about 75 μm diameter and 50 μm thickness, is sandwiched between the diamond anvils and contained within a hole drilled into a metallic gasket. The opposite diamond anvil is a designer anvil with a five-turn microcoil. One end of this microcoil is attached to a connection pad located on the side of the anvil, and the other end of the microcoil emerges from the diamond surface in order to make electrical contact to the gasket. Electrical

Downloaded 04 Apr 2003 to 128.115.60.31. Redistribution subject to AIP license or copyright, see http://ojps.aip.org/rsio/rsicr.jsp

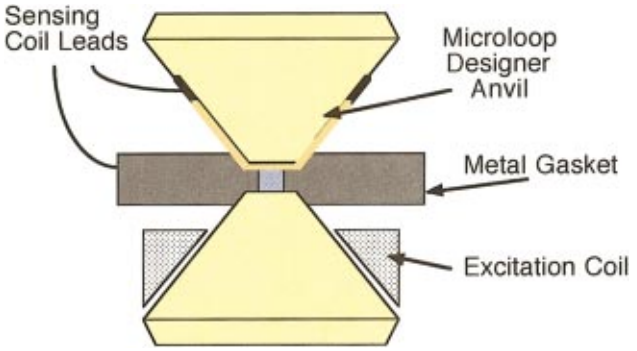

FIG. 4. (Color) Arrangement specific to designer diamond anvils used for ac susceptibility in which the sensing coil is located on the top diamond, and the 55-turn excitation coil is wrapped directly around the bottom diamond. The sensing coil protrudes through the culet and is grounded through the metal gasket.

wires are attached to the tungsten connection pads with silver paint, and spot wielded to the gasket. The signal voltage is then directed to a lock-in amplifier by means of a shielded, twisted pair cable. A nonmagnetic, Be–Cu diamond anvil cell is used in these experiments (Kyowa Seisakusho Co., Ltd., Japan).

A schematic of the circuit is shown in Fig. 5. The excitation coil is driven by a sine wave from a function generator (Stanford Research Systems, DS360). Frequencies from 100 Hz to 10 kHz have been used with good results. The excitation coil and the sensing microcoil are located on opposite sides of the metal gasket, so special care must be taken to ensure that the penetration skin depth of the excitation field is large relative to the thickness of the gasket.

Typical excitation currents are 10–90 mA, which yield ac magnetic excitation fields up to about 6 G. The voltage induced in the sensing coil is fed to a lock-in amplifier (Stanford Research Systems, SR850). The real part of the magnetic susceptibility corresponds to the voltage signal component which lags the reference signal by 90°. Due to the intrinsically high signal-to-background ratio of the microcoils, no background compensation coil or compensation circuits are needed.

B. Cryogenics

In order to collect magnetic susceptibility data as a function of temperature, we use a closed cycle He cryostat (Cryomech ST15), which allows us to cool the DAC from room temperature down to 10 K. Due to the slow cooling rate (approximately 2.4 deg/min), we typically collect data as the cryostat cools down. Two Si diode sensors are used to monitor the temperature within the cryostat, one located on the body of the DAC in order to monitor the sample temperature, and a second located on the cryostat cold head that is used for temperature stabilization.

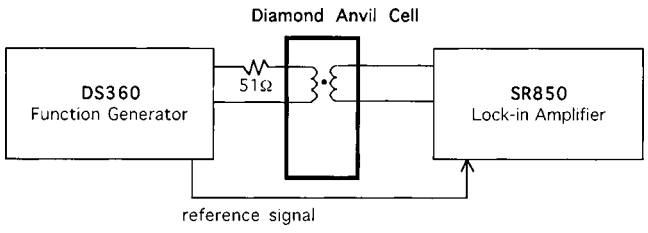

FIG. 5. Schematic of the circuit for ac susceptibility.

Due to the thermal contraction of the Be–Cu DAC, the pressure is not constant as the temperature changes. Cooling from 300 K down to 10 K can result in a 60% increase in sample pressure if the DAC is not compensated for thermal contraction. It is therefore important to monitor the pressure within the DAC as a function of temperature. This is performed by measuring the ruby fluorescence of a ruby chip in the sample region of the DAC.[16] Laser light is coupled to the ruby using a 532 nm laser focused on the ruby within the DAC, and the spectrum is measured using a Princeton Instruments charge coupled device (CCD). In order to determine the pressure at a given temperature, we first measured the ambient pressure redshift of the $R_1(T)$ line throughout our accessible temperature range, which agreed with the published results within experimental error.[17] The pressure was then calculated using the technique of Ragan *et al.*,[18] in which the pressurized blueshift of the $R_1(T)$ peak is compared with the ambient pressure result. In order to obtain a more constant $P(T)$ relationship, we include a Delrin O ring inside the DAC which counteracts thermal contraction of the Be–Cu DAC body, and results in only a 20% increase in sample pressure upon cooling from room temperature to 10 K.

C. Measurements with a Gd sample

Pressure induced phase transformations in rare earth metals are of great interest because of the possibility of observing such phenomena as a volume collapse transition associated with delocalization of the $4f$ shell, or a Mott transition in this class of materials. In addition, magnetic ordering transitions, which are well documented at low temperatures, are easily altered by application of high pressure. We study gadolinium as a test case for this newly developed designer diamond anvil technique to investigate the magnetic ordering temperature at high pressure.

Gadolinium undergoes a ferromagnetic transition at $T_c = 293\,\mathrm{K}$ at ambient pressure,[19] which is depressed with the application of pressure. Therefore, for our preliminary test experiments, we studied a Gd sample (Alfa Æsar, 99.9%) with a diameter of approximately 75 μm and a thickness of about 50 μm. A typical result for the real susceptibility, χ', with a frequency of 1 kHz and a pressure of 1.6 GPa is shown in Fig. 6. Initially, at high temperatures, Gd is paramagnetic, but as the temperature is lowered, it undergoes a ferromagnetic transition which is accompanied by a large increase (approximately 4% above the background) in the signal. The Curie temperature was determined by the location of the peak in $-d\chi'/dT$, which was found to be 274 K. The temperature at which this large increase in χ' occurred was found to linearly decrease in temperature as the pressure was increased (see the inset in Fig. 6). The rate of the decrease in the Curie temperature was determined to be $dT_C/dP = -14 \pm 2$ K/GPa, which is in good agreement with previous results ranging from -12 (Ref. 20) to -17 K/GPa.[21]

Downloaded 04 Apr 2003 to 128.115.60.31. Redistribution subject to AIP license or copyright, see http://ojps.aip.org/rsio/rsicr.jsp

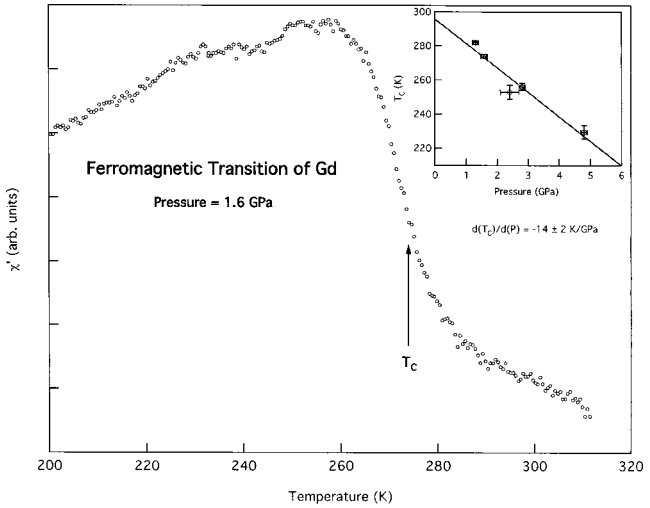

FIG. 6. Magnetic susceptibility of a Gd sample taken at 1.6 GPa with a microloop designer anvil. The ferromagnetic transition at $T_C = 274$ K is clearly observable in the data. The inset shows the linear decrease in T_C of -14 K/GPa.

IV. DISCUSSION

We find that the multiloop designer anvil technique offers exceptional performance with regard to signal sensitivity and the signal-to-background ratio. One obvious idea for improving the performance of the sensing microcoil is to increase the number of turns. Since our projection lithography process is capable of 1 μm linewidths, the number of turns in the microcoil pattern can be increased from 5 to 50, allowing it to capture approximately as much flux as a 1000-turn external coil. However, a close examination of the circuit design reveals that there are no great advantages to doing this. As mentioned previously, increasing the number of turns in the sensing coil does not increase the signal-to-background ratio. Furthermore, increasing the number of turns has the secondary effect of also increasing the microcoil's resistance and, hence, the thermal Johnson noise associated with the coil. Our five-turn sensing microcoils have a resistance of approximately 1.7 kΩ. The Johnson noise associated with it is then V_{noise} [root mean square (rms)]$=(4k_BTRB)^{1/2}$, where k_B is the Boltzmann constant, T is the temperature, and B is the frequency bandwidth in hertz. At room temperature, the Johnson noise of the microcoil is then $V_{\text{noise}}(\text{rms}) = 5.3\,\text{nV/Hz}^{1/2}$, which is comparable to the input noise of 5 $\text{nV/Hz}^{1/2}$ of the SR850 lock-in amplifier. The overall noise input at the input of the SR850 is then $(5^2+5.3^2)^{1/2} = 7.3\,\text{nV/Hz}^{1/2}$. Since the Johnson noise of the microcoil is already comparable to the input noise of the SR850 lock-in, any further increases in the number of turns and resistance of the microcoil will not significantly improve the overall signal to noise of the microcoil/lock-in system. We see, then, that although the signal voltage can be increased by increasing the number of turns, neither the signal-to-background ratio nor the signal-to-noise ratio is appreciably improved.

The maximum sensitivity of our experiments is primarily limited by the thermal noise in the lock-in amplifier and in the microcoil itself. Microcoil signals below about 1 nV will tend to be obscured by this intrinic system noise. It is possible, however, to boost the signal voltage by increasing the amplitude and/or the frequency of the magnetic excitation field. By doubling the number of turns in the excitation coil and by increasing the frequency up to 90 kHz, we can reasonably expect to increase the sensitivity of our system to measure volume susceptibilities down to the 10^{-3} emu/cm^3 range, or possibly even smaller, for a standard 75 μm diam sample. Further increasing the measurement sensitivity beyond this range is likely to be hampered by the fact that the gasket itself contributes a small magnetic susceptibility signal to the background. Further experimentation will be needed to investigate all these issues.

In conclusion, we find that the microloop designer anvil approach offers an attractive method for performing high-pressure magnetic susceptibility experiments due to its outstanding signal-to-background ratio as well as its relative ease of use. With the designer anvil approach, the sensing coil can be optimally sized and positioned with respect to the sample in order to maximize the signal while minimizing the background. This intrinsically low background level is a valuable feature for any future magnetic susceptibility experiments that involve magnetic phases and phenomena which have much smaller characteristic signals than current DAC techniques allow.

ACKNOWLEDGMENTS

The authors would like to thank Dave Ruddle and Alan Frank for their generous help throughout this project. The authors also thank Dino Ciarlo and Ron Lee for helpful discussions. Much technical assistance was provided by Steve Falabella, and they thank L. T. Wiley, B. T. Goodwin, and J. Akella for support of this work. This work was performed under the auspices of the U.S. Department of Energy by the University of California, Lawrence Livermore National Laboratory, under Contract No. W-7405-Eng-48.

[1] A. Jayaraman, Rev. Mod. Phys. **55**, 65 (1983).
[2] A. Jayaraman, Rev. Sci. Instrum. **57**, 1013 (1986).
[3] M. Eremets, K. Shimizu, T. Kobayashii, and K. Amaya, Science **281**, 1333 (1998).
[4] K. Shimizu *et al.*, Nature (London) **393**, 767 (1998).
[5] Y. Timofeev *et al.*, Rev. Sci. Instrum. **73**, 371 (2002).
[6] E. Gregoryanz *et al.*, Phys. Rev. B **65**, 64504 (2002).
[7] M. Ishizuka, K. Amaya, and S. Endo, Rev. Sci. Instrum. **66**, 3307 (1995).
[8] M. Ishizuka, K. Amaya, and S. Endo, Phys. Rev. B **61**, R3823 (2000).
[9] S. Weir *et al.*, Appl. Phys. Lett. **77**, 3400 (2000).
[10] S. Catledge, Y. Vohra, S. Weir, and J. Akella, J. Phys.: Condens. Matter **9**, 67 (1997).
[11] J. Patterson *et al.*, Phys. Rev. Lett. **85**, 5364 (2000).
[12] B. McWilliams *et al.*, Appl. Phys. Lett. **43**, 946 (1983).
[13] V. Malba, V. Liberman, and A. Bernhardt, Int. J. Microcircuits Electron. Packag. **20**, 371 (1997).
[14] Y. Timofeev, H. Mao, V. Struzhkin, and R. Hemley, Rev. Sci. Instrum. **70**, 4059 (1999).
[15] S. Klotz, J. Schilling, and P. Muller, in *Frontiers of High-Pressure Research*, edited by H. Hochheimer and R. Etters (Plenum, New York, 1991), pp. 473–484.
[16] H. Mao, P. Bell, J. W. Shaner, and D. Steinberg, J. Appl. Phys. **49**, 3276 (1978).
[17] W. Vos and J. Schouten, J. Appl. Phys. **69**, 6744 (1991).
[18] D. Ragan, R. Gustavsen, and D. Schiferl, J. Appl. Phys. **72**, 5539 (1992).
[19] J. Coey, V. Skumreyev, and K. Gallagher, Nature (London) **401**, 35 (1999).
[20] L. Patrick, Phys. Rev. **93**, 384 (1954).
[21] D. McWhan and A. Stevens, Phys. Rev. **139**, A682 (1965).

Downloaded 04 Apr 2003 to 128.115.60.31. Redistribution subject to AIP license or copyright, see http://ojps.aip.org/rsio/rsicr.jsp